Journal of The Electrochemical Society, **149** (3) H81-H86 (2002)
0013-4651/2002/149(3)/H81/6/$7.00 © The Electrochemical Society, Inc.

Effects of Oxygen Partial Pressure and Annealing Temperature on the Formation of Sputtered Tungsten Oxide Films

C. Bittencourt,[a] R. Landers,[a] E. Llobet,[b,z] G. Molas,[b] X. Correig,[b] M. A. P. Silva,[c] J. E. Sueiras,[d] and J. Calderer[e]

[a]*Instituto de Física "Gleb Wataghin," Universidade de Campinas, 13083-970 Campinas, SP, Brazil*
[b]*Departament d'Enginyeria Electrònica, Universitat Rovira i Virgili, Campus Sescelades, 43007 Tarragona, Spain*
[c]*Instituto de Física de São Carlos, Universidade de São Paulo, 16000-000 São Carlos, SP, Brazil*
[d]*Departament d'Enginyeria Química, Universitat Rovira i Virgili, Campus Sescelades, 43007 Tarragona, Spain*
[e]*Departament d'Enginyeria Electrònica, Universitat Politècnica de Catalunya. Campus Nord, 08034 Barcelona, Spain*

Thin films of tungsten oxide were deposited on silicon substrates using reactive radio frequency sputtering. The structure of the films strongly depends on the conditions of deposition and post-treatment. Important issues are the influences of oxygen pressure during deposition and annealing temperature on the morphology. Atomic force microscopy and scanning electron microscopy revealed that films were formed by grains. The sample deposited with an Ar:O_2 partial pressure ratio of 1:1 showed the highest roughness and the smallest grains when annealed at 350°C. X-ray photoelectron spectroscopy analysis revealed that the films were close to their stoichiometric formulation irrespective of the oxygen partial pressure used during film deposition. The number of W=O bonds at the grain boundaries was found to be dependent on the oxygen partial pressure. Analysis by Raman spectroscopy suggested that the structure of the films was monoclinic. On the basis of these results, an annealing temperature of 350°C was selected as post-treatment for the fabrication of WO_3 gas sensors. These sensors were highly sensitive, highly selective to ammonia vapors, and moderately responsive to humidity.
 [DOI: 10.1149/1.1448821]

Manuscript submitted February 26, 2001; revised manuscript received October 24, 2001. Available electronically February 8, 2002.

The last few years have seen a growth in worldwide concern for global environmental protection and governments have introduced a set of antipollution measures. Any serious attempt to control pollution requires the emission of hazardous gases into the atmosphere to be continuously monitored. For this purpose, solid-state gas sensors[1,2] have proved to be very promising. In resistive devices, gases are sensed by how they affect the electrical conductance of a chemically sensitive layer, such as metal-oxide semiconductors (MOSs)[3] and conducting polymers.[4]

To detect small concentrations of a reactive gas in air, metal oxide sensors rely on changes in the value of the conductance of the sensitive layer. These changes are caused by the gas altering the equilibrium condition of the carrier density reached in the presence of air.[5] The mechanism mainly responsible for conductance changes involves variations in the concentration of surface oxygen adsorbates.[5] The formation of adsorbates such as O^- and O^{2-} at the metal-oxide surface by its interaction with air, abstracts electrons from the film. The adsorbates can thus be thought of as a trap for electrons. The trapping of electrons by the adsorbates, causes a depletion of carriers at the surface and a potential barrier to charge transport develops. With films whose morphology is granular, a depletion of carriers and a potential barrier occur at the grain boundaries. Both carrier depletion and potential barrier lead to high resistance intergrain contacts, which dominate the conductance of the sensors.[6] Therefore, any gas that reacts altering the quantity of charge trapped at the surface of the metal-oxide active layer can be detected.

Among MOSs, tungsten oxide is a promising material for gas sensing. Several studies have shown that it can be used for the detection of nitrogen oxides (NO and NO_2), carbon monoxide, ammonia vapors, and hydrocarbons.[7-9] Tungsten oxide films can be deposited by reactive radio frequency (rf) sputtering, thermal evaporation, drop coating, sol-gel methods, and screen printing. The morphology of these films, which are usually comprised of O-W-O grains with terminal W=O at the surface,[10] is influenced by deposition methods and post-treatment. Surface oxo-groups (W=O) in some metal oxides were identified to dehydrogenation active centers.[11] These centers apparently play an important role in the adsorption of NH_3 and dissociation of hydrocarbons,[11-13] *i.e.*, in the sensing behavior of the films.

For a WO_3-based sensor, which behaves as an n-type semiconductor with fully ionized donors at typical working temperature, the electrons that are trapped by oxygen adsorbates come from the conduction band. At working temperatures in the presence of a reactive gas, surface catalyzed combustion may occur, and so the surface coverage of oxygen adsorbates may decrease. The reduction in number of oxygen adsorbates releases electrons back into the conduction band. This causes the film conductance to increase as a consequence of the reductions in the surface potential barrier to change transport.[3]

As we have discussed above, in films with granular morphology like WO_3 films, the gas is sensed at the boundaries of the grains. To achieve a better understanding of the processes involved in the electronic behavior of the film, it is therefore important to have information about the grains. The aim of this article is to report how the oxygen partial pressure in the Ar-O_2 gas mixture used to deposit the samples and the temperature of annealing affect the grain size of sputtered WO_3 films and the formation of W=O bonds at the grain boundaries, both quantities are very important in the sensing behavior of the films.[6,11-13]

Scanning electron microscopy (SEM) and atomic force microscopy (AFM), which have outstanding potential in film analysis, was employed to characterize the morphology of the WO_3 films. Their composition was analyzed by X-ray photoelectron spectroscopy (XPS). Raman scattering measurements were carried out to identify the nanocrystallization of the WO_3 films and the evolution of the W=O bonds for the different deposition parameters and annealing temperatures. Finally, gas sensors were produced using rf sputtered WO_3 films deposited onto a microelectronic substrate that included a pair of interdigitated gold electrodes and a NiCr resistive heater (more details on the substrate design are given elsewhere[9]). The gas-sensing properties of these devices were investigated.

Experimental

The tungsten trioxide films were prepared by a reactive rf sputtering system. A target of 99.95% purity with diam of 100 mm and

[z] E-mail: ellobet@etse.urv.es

thickness of 0.125 in. was used. The target substrate distance was fixed at 70 mm. The silicon substrates were held in thermal contact with a holder during the deposition. The substrate temperature was kept constant during film deposition at room temperature. The sputtering atmosphere consisted of Ar-O_2 mixed gas and its flow rate was controlled by separate gas flowmeters to tailor the Ar:O_2 gas percentage in the chamber [sample S1 (10:5), sample S2 (0:10), sample S3 (5:10), and sample S4 (1:1)]. The pressure in the chamber during deposition was 5×10^{-3} mbar.

After deposition, the samples were annealed in dry air from 200 to 450°C in steps of 50°C that lasted 3 h. After each step, all the samples were analyzed. The resulting surface composition was determined by XPS. The XPS measurements were performed with a system equipped with a hemispherical electron energy analyzer. The photon source was a nonmonochromatized Al Kα line ($h\nu = 1486$ eV). The resolution of the system (source + analyzer) was 1 eV.

The evolution of the W=O and the crystallization of the films for each temperature step was analyzed by Raman spectroscopy. The Raman spectra of these films were recorded at room temperature using a Spex 1403 1 m double pass spectrometer equipped with a cooled low noise photomultiplier tube using the 330 nm laser line of an Ar laser. The laser power focused onto the sample was 0.26 mW. The resolution of the Raman spectrum is 5 cm^{-1}. The surface morphology and homogeneity of the samples were investigated with a JSM6400 SEM operated at 30 keV, with an energy dispersive X-ray spectroscopy (EDX) detector and an AFM accomplished in a Nanoscope III (Digital Instruments) using a triangular shaped (0.06 N/m) Si_3N_4 cantilever tip in contact mode.

To investigate the gas sensing properties of the films, the sensors were introduced into a thermally controlled test chamber (±1°C). All contaminants and water (to reach the required level of moisture) were injected into the test chamber by high precision chromatographic syringes. Dry air was used both as a reference gas and as a diluting gas to obtain the desired concentrations of the test gases. These were 0-1000 ppm ammonia, 0-1000 ppm benzene, 0-10000 ppm methane, 0-1000 ppm ethanol, and water vapor [20-80% relative humidity (RH)]. The procedure for creating the desired concentration in the test chamber is described elsewhere.[14] The electrical resistance of the sensors was monitored, acquired, and stored in a PC using a commercial acquisition data board and written-in-house control software.

Results and Discussion

XPS.—The XPS results after each annealing step showed that there was no substantial change in the composition of the films, so we present only those recorded after the final annealing step (450°C). We observed that all structures in the XPS spectra were shifted by 2.5 eV toward higher energy, which indicates charging effects. The composition of the films was analyzed by XPS. We observed that when the WO_3 films were exposed to Ar^- ion bombardment, this caused reduction to WO_x species. Therefore, for composition analysis, we recorded spectra for different photoelectron collection angles (PCA). This is the angle between the electron energy-analyzer and the angle normal to the sample surface. For the XPS system used, the depth below the surface that can be probed goes from approximately 80 to 20 Å when the PCA varies from 0 to 80°.

The XPS spectra recorded on all samples using PCA equal to 0°, *i.e.*, when the photoelectrons are generated in the deepest region that can be probed, were similar to a typical WO_3 spectrum. Figure 1 shows the W 4f and O 1s core level spectra recorded on sample S4 after the annealing step at 450°C. The W 4f core level spectrum shows the two components associated with the W $4f_{7/2}$ and $4f_{5/2}$ spin-orbit doublet. Its binding energy, E_b is close to the characteristic E_b of the tungsten atom in WO_3 stoichiometric films. The O 1s peak is situated 494.8 eV above the W $4f_{7/2}$ core level line. This relative peak position is in agreement with the value reported for

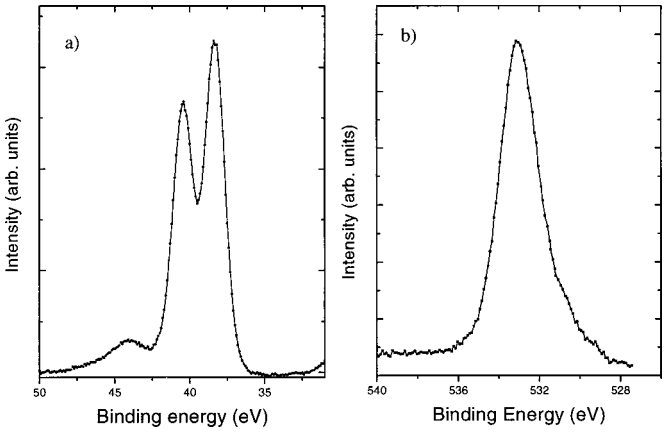

Figure 1. XPS recorded at an angle of 0° on sample S4 after the 450°C annealing step. (a) The 4f core level spectrum, and (b) the O 1s core level spectrum.

WO_3 stoichiometric films.[15] There is a tail toward lower energy associated with the O 1s peak in the O 1s spectrum (Fig. 1b). Its origin is discussed later in this paper. Quantitative analysis of the oxygen-to-tungsten atomic ratio, made with data from the XPS spectra recorded on the samples, shows that the WO_3 films are close to their stoichiometric formulation. This shows that with the oxygen partial pressures used for the deposition of the films, no change in the incorporation of oxygen atoms can be detected.

The O 1s core level spectra recorded on the films using a PCA of 50°, *i.e.*, when the technique becomes more sensitive to the surface, showed an additional structure. Figure 2 shows the spectrum recorded on sample S4 using a PCA of 50°. The O 1s core level spectrum recorded near the surface is made up of two structures, one of which is generated by photoelectrons emitted from oxygen atoms in WO_3 (O-W-O) at 533 eV and the other is situated 2 eV below this one. This relative peak position suggests that the second structure is generated by the photoelectrons emitted from oxygen atoms located at W=O bonds.[16] The W 4f core level spectrum recorded using a PCA of 50° was similar to the one recorded with a PCA of 0° but there was an increase in its width. This increase can be associated with the existence of tungsten atoms in different environment, *i.e.*, located in W=O and W-O bonds.

We can now address the previously mentioned tail of the O 1s peak recorded with a PCA of 0° (Fig. 1), to be due to the photoelectrons emitted from oxygen atoms located at W=O bonds. Its intensity is small because the contribution to the spectrum made by the number of photoelectrons emitted from oxygen atoms at W=O bonds is small when compared to the contribution made by the number of photoelectrons emitted from oxygen atoms at W-O bonds. The small intensity of this structure may suggest that W=O bonds are mainly at the surface.

The spectrum recorded on sample S4 with a PCA of 80°, *i.e.*, the highest sensitivity to the surface, mainly showed the structure associated with photoelectrons emitted from oxygen atoms at W=O bonds. Figure 3 shows that the structure associated with photoelectrons emitted from oxygen atoms at W-O bonds appears just as a tail on the high energy side. As the possibility of contamination can be ruled out, these results support the previous suggestion that the sample surface is mainly formed by W=O bonds.

The XPS spectra recorded on the other samples (S1, S2, and S3) behaved in a similar way, but the relative intensity between the two components in the O 1s core level spectrum (W=O/O-W-O) increased as O_2 partial pressure in the Ar-O_2 gas mixture increased. Although there was no change in the chemical composition of the samples as O_2 partial pressure in the mixture used for deposition increased, the availability of oxygen in the mixture produces a

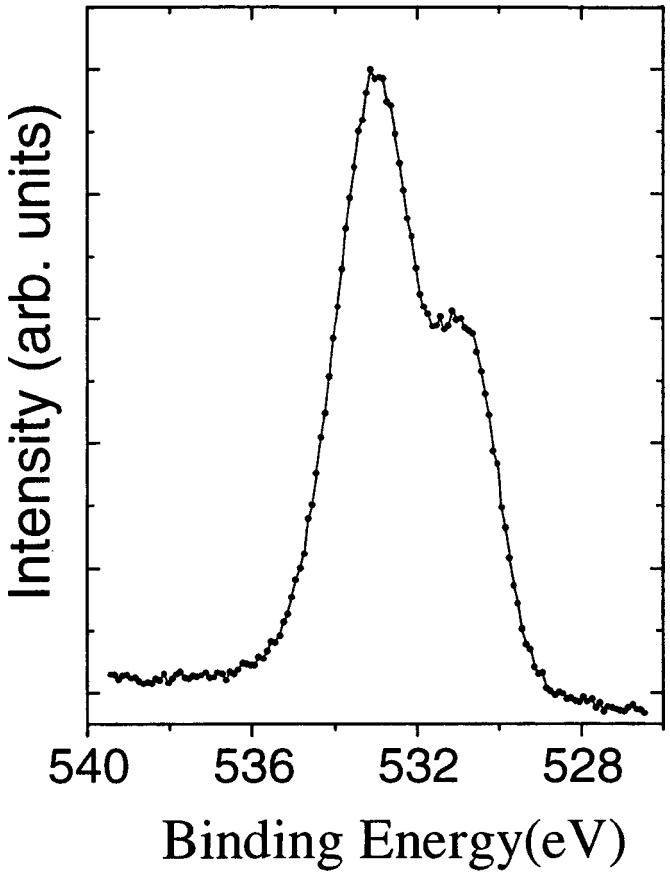

Figure 2. Detailed XPS scan O 1s core level spectrum of the sample S4 recorded at an angle of 50°. The spectrum was recorded after the 450°C annealing step.

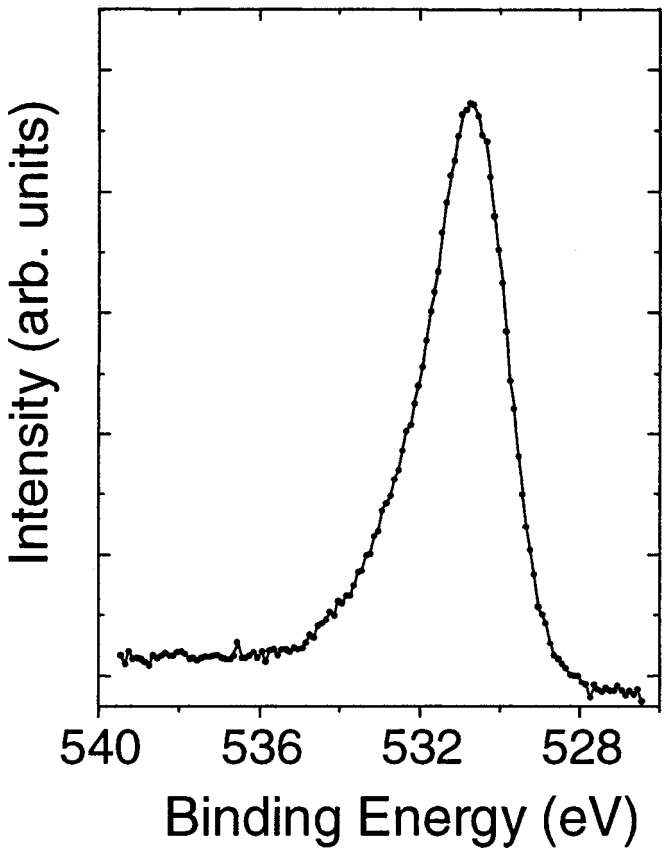

Figure 3. Detailed XPS scan O 1s of the sample S4 recorded at an angle of 80°. The spectrum was recorded after the 450°C annealing step.

more oxygenated surface, and the oxygen atoms are located at the W=O bonds.

Raman spectroscopy.—Raman measurements were performed because this technique is known to provide the "fingerprint" of WO_3 film.[17] Figure 4 shows the Raman spectra of the tungsten trioxide samples (S1, S2, S3, and S4) as grown. The as-grown films appeared to be amorphous. The band around 550 cm^{-1} is associated with the silicon substrate. The spectra show two broad bands, one of which in the 200-400 cm^{-1} region peaking around 275 cm^{-1} and the other in the 600-900 cm^{-1} region peaking around 800 cm^{-1}. These are followed by a peak at around 950 cm^{-1}. Figure 4 shows that the bands of the Raman spectrum of sample S4 are narrower than those of the spectra recorded on the other samples. This may suggests that the percentage of Ar-O_2 used during the deposition of sample S4 improved the crystallinity of the film.

The spectra recorded after each annealing step showed mainly that the bands become narrower, which reflects an increase in the crystallinity of the films. Figure 5 shows how the Raman bands evolved as annealing temperature increased for sample S4. Film crystallinity was noticeably increased after the 350°C annealing step. This trend was the same for all samples. The two broad bands in the spectra recorded on the as-grown film (see Fig. 4) had split in peaks located at around 270 and 330 cm^{-1} and 715 and 807 cm^{-1}. Also, the intensity of the band at 950 cm^{-1} decreased. Comparing the Raman spectra recorded on the samples after each annealing step with spectra for different WO_3 phases[18] suggests that the films deposited after annealing at 350°C are monoclinic in structure. This structure of the tungsten oxide film consists of a packed corner-shared WO_6 octahedron units that form clusters. This film is formed by O-W-O microcrystalline grains connected to each other by W-O-W or hydrogen bonds through water bridges, with terminal W-O bonds at the surface of the grains.[18] The two Raman peaks at 715 and 807 cm^{-1} were assigned to O-W-O modes, and the one at 950 cm^{-1} to a W=O stretching mode.[18] The additional peaks at 270 and 330 cm^{-1} are due to the bending vibration δ(O-W-O).[19]

It has been reported[19] that the ratio of integrated Raman scattering intensities of the W-O band to that of the O-W-O band in the region of 600 to 900 cm^{-1} can be used to measure the relative cluster size. The number of W-O terminal bonds around the cluster is inversely proportional to the size of the cluster.

Figure 6 shows the typical annealing temperature dependence of the Raman intensity ratio of W=O/O-W-O for these films. The W=O/O-W-O ratio decreases as the temperature of annealing increases. This shows that, for these films, increasing the annealing temperature increases the size of the cluster, *i.e.*, decreases the number of W-O bonds.

Irrespective of the oxygen partial pressure used during film deposition, the XPS analysis reveals that the films were close to their stoichiometric formulation, and the main difference among the Raman spectra is in the intensity of the peak related to the W=O bonds. This suggests that the main effect of changing the O_2 partial pressure in the range that we analyzed is a change in the morphology of the films, *i.e.*, the size of the clusters, not their chemical composition.

Structural characterization.—To understand how the annealing temperature affects the morphology of the WO_3 samples, a structural characterization based on the electron microscopy analysis and AFM were performed.

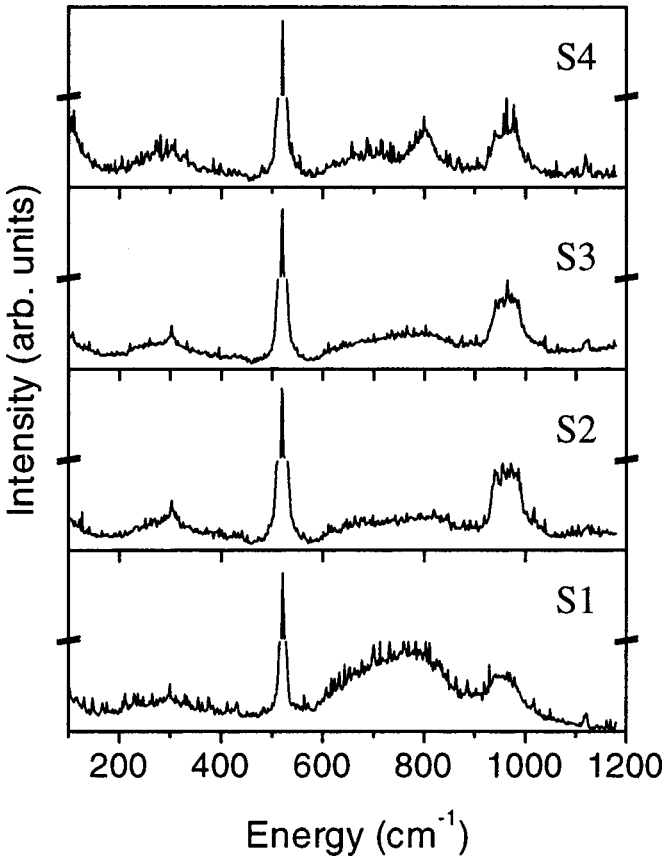

Figure 4. Raman spectra of as grown WO_3 samples.

The as-grown films showed an amorphous textured layer covering the Si substrate. The micrographs, recorded on the samples after each annealing step, showed a structural evolution of the films. Annealing at 200°C caused WO_3 grains to form. As annealing temperature increased, the average size of the grains increased. This increase in grain size is in agreement with the Raman results, which also showed that around 350°C there was a noticeable improvement in the crystallinity of the films. All samples had the same behavior. AFM gives the direct measurement of the grains; sample S4 was the one with the smallest grain after being annealed at 350°C. Figure 7 shows the AFM micrograph recorded on sample S4 annealed at 350°C. It is essentially inhomogeneous, and is made up of grains and voids. The voids within the film structure provide direct conduits for oxygen and gas molecules to flow in from the environment. EDX analysis showed that the grains and the bottom of the voids contained tungsten (the equipment used was not suitable for detecting the presence of oxygen). Therefore, if EDX and XPS results are taken into account, it can be derived that sample S4 is a porous tungsten oxide film.

Gas-sensing properties.—The response of sputtered WO_3 sensors to ammonia, ethanol, benzene, and methane was investigated. Sensitivity was defined as the ratio R_a/R_g, where R_a is the static sensor resistance in dry air and R_g is the static sensor resistance in the presence of gas. AFM showed that annealing at 350°C leads to a film that is made up of WO_3 grains (see Fig. 7). Raman results show that after annealing at this temperature, the films were not amorphous. Moreover, from both analyses, we can conclude that the films were polycrystalline. For sensing purposes, polycrystallinity and small grains are advantages because they lead to films with high surface areas for the gas to interact with.[3] On the basis of the results found by XPS, AFM, and Raman spectroscopy, the sensors were annealed at 350°C for 24 h.

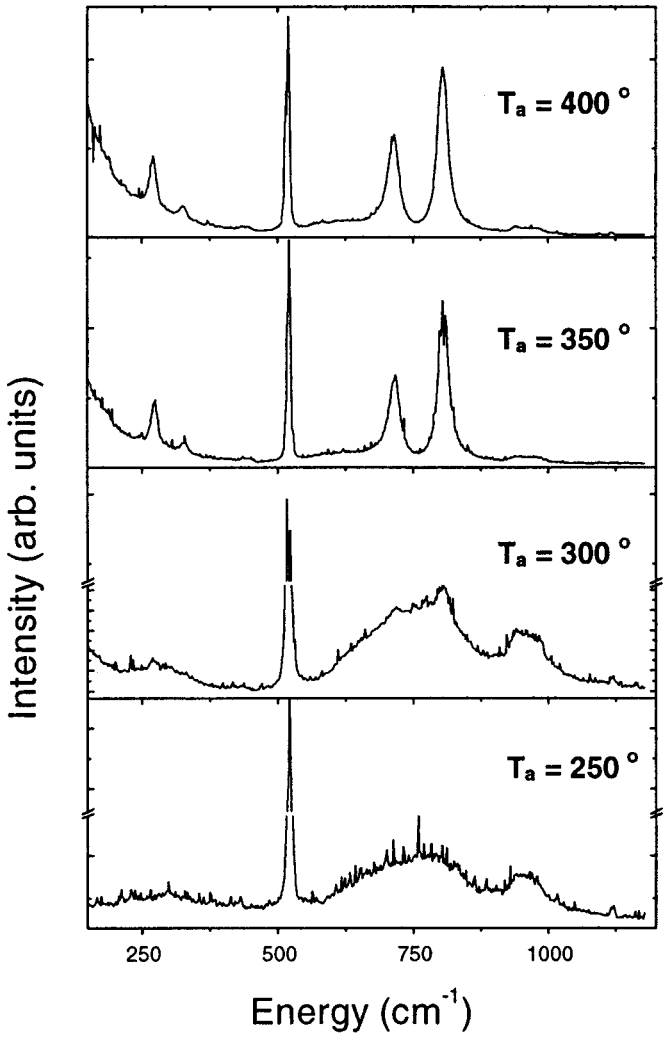

Figure 5. Raman spectra of sample S4 after each annealing step.

Figure 8 shows a typical response of the fabricated sensor (sample S4) to increasing concentrations of ammonia vapor. Sensitivity to ammonia was highest when the sensors were operated at 250°C. Sensitivity was best for the sensor fabricated with an Ar:O partial pressure ratio of 1:1. AFM micrographs showed that the grains of this sample were smaller than all the others when annealed at 350°C. Small grains are important because they lead to a high surface area, which in turn enhances gas sensitivity. The response time of the sensors in the presence of ammonia (measured between 10 and 90% of the variation in sensor resistance) was typically 25 s. When the sensors were exposed to dry air after being exposed to ammonia, baseline resistance was reached in about 50 s. Figure 9 shows the sensitivities of sensor S4 to ammonia and ethanol when operating at different temperatures. The sensitivities to the other gases studied are not shown because the sensors (for all samples) were almost completely insensitive to them. Figure 9 shows that the sensor is very selective to ammonia when operating at 250°C.

Sensing mechanism in WO_3 sensors.—In n-type semiconductor sensors, the current is carried by conduction band electrons, and sensor conductivity increases in the presence of a reducing gas. WO_3 is an n-type semiconductor, so there will be more carriers when the surface coverage of oxygen is decreased by the presence of a reducing species such as ammonia. This increases conductivity.

A simple model to explain the interaction of a reducing species such as NH_3 with the sensing film is the following: The concentration of the adsorbed oxygen ions on the metal oxide surface is de-

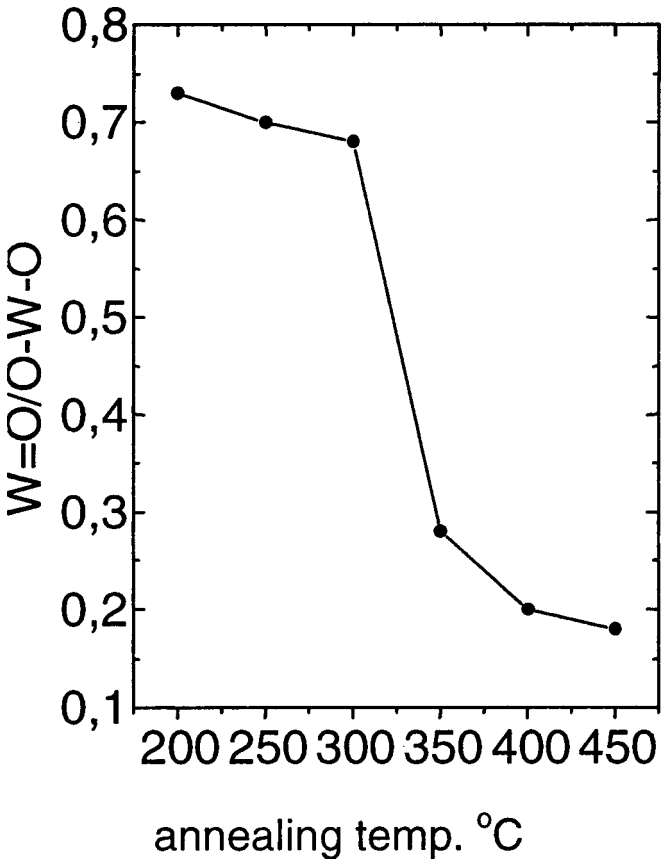

Figure 6. Typical anneal temperature dependence of the Raman intensity ratio of W=O/O-W-O for the analyzed WO_3 films.

creased by the reducing gas. The depletion region diminishes, and the conductivity of the metal oxide rises correspondingly. If the adsorption of molecular oxygen creates negatively charged oxygen ions on the surface

$$3/2\ \ O_2(\text{gas}) + 3/2e^- = 3/2\ \ O_2^-(\text{surface}) \qquad [1]$$

then the electron affinity of the metal oxide, and thus the band interval, remain unchanged. The change in conductivity is solely due to the space-charge region created in the metal oxide by the negative charge of the surface.

Semireaction 1 has two steps: the physisorption of O_2 on WO_3, and the charge transfer from the surface to the adsorbate. The creation of positive ions from reducing gases on the surface

$$2NH_3(\text{gas}) = 2NH_3^{3/4+}(\text{surface}) + 3/2e^- \qquad [2]$$

creates an electron enhancement region, which causes a corresponding rise in conductivity.

As before, semireaction 2 has the two steps of physisorption and charge transfer, but this time from NH_3 to the surface.

The formation of N_2 and H_2O is expected because NH_3 behaves as a mild reducing agent. Therefore, the overall Reaction 3 is produced by adding semireactions 1 and 2

$$2NH_3(\text{gas}) + 3/2\ \ O_2(\text{gas}) = [(2NH_3^{3/4+})(3/2\ \ O_2^-)]\text{surface}$$
$$= N_2 + 3H_2O \qquad [3]$$

Reaction 3 has three steps: the surface diffusion of charged species, the ionic bond formation of the complex, and the desorption of the reaction products N_2 and H_2O.

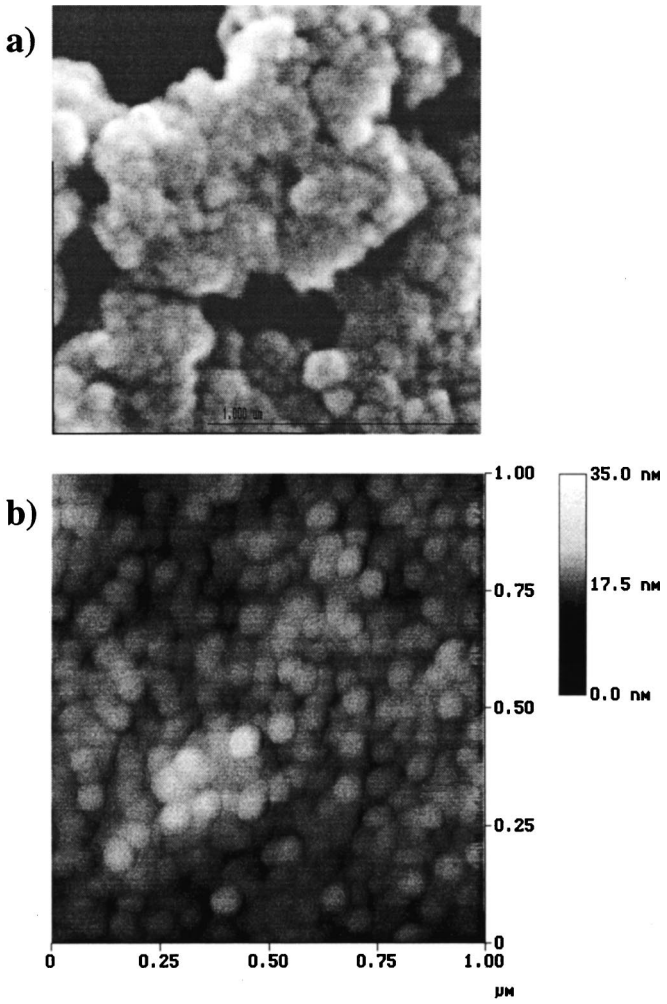

Figure 7. SEM and AFM micrographs showing the morphology of sample S4 annealed at 350°C.

According to Gerblinger *et al.*,[20] the creation of this surface complex, whether it is charged or not, changes the bonding relationships on the surface of the metal oxide, *i.e.*, the coordination of the metal by oxygen ions or the bond lengths between the ions. This changes the electronegativity (bandgap) of the metal oxide. The narrowing of the bandgap creates an accumulation region, and increases

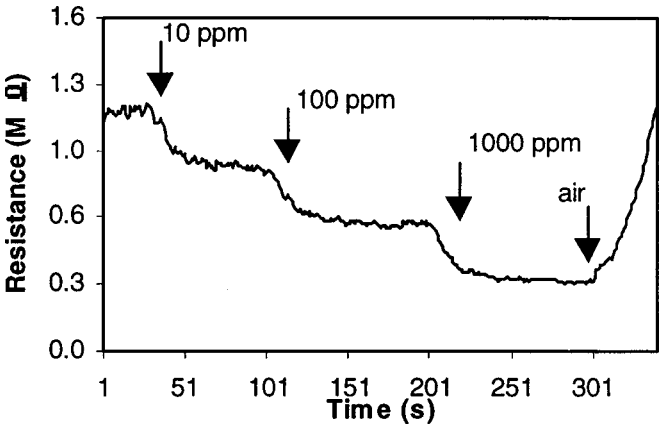

Figure 8. Typical response curve of a sputtered WO_3 gas sensor to successively increased concentrations of ammonia vapors.

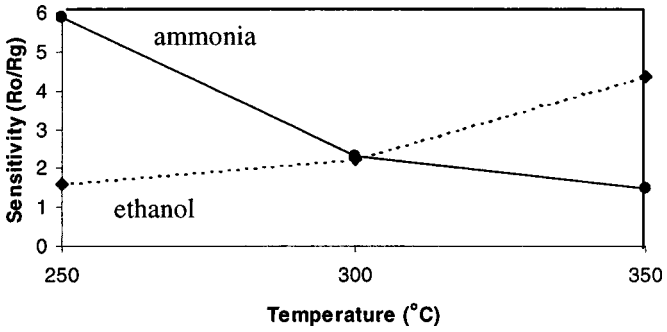

Figure 9. Sensitivity to ammonia and ethanol vapors of gas sensor (S4) as a function of the operating temperature.

both the space-charge region in n-type semiconductors such as WO_3, and conductivity. The effects of changing the bandgap superimpose on those caused by the space-charge region due to surface charge.

This model explains how WO_3 behaved at 250°C or under. The lower sensitivity of our sensors when operated at 300°C may be due to the spontaneous decomposition of NH_3 into N_2 and H_2 on the sensor surface before its adsorption and the subsequent reaction with oxygen.[21,22].

On the other hand, increasing the working temperature increased sensitivity to ethanol (see Fig. 9). This may be because the temperature needed for the catalyzed combustion of ethanol is higher.

Response to water vapor.—Moisture may be adsorbed onto the sensor surface, and this increases the active film conductance (in n-type semiconductors). Therefore, water vapor may cause interference with other gases. Figure 10 shows the typical response of a sputtered tungsten oxide sensor (sensor S4) operating at 250°C, when the moisture level was increased from 15 to nearly 80% RH. The change in baseline resistance due to humidity was lower than the change in the baseline resistance of commercial sensors based on tin-oxide [*e.g.*, Toguchi gas sensor (TGS)-type]. Increasing the working temperature of the sensor enhanced its sensitivity to water vapor.

Conclusions

A set of tungsten trioxide films were prepared by rf sputtering using different $Ar:O_2$ gas percentages. AFM and SEM revealed that films were formed by grains. XPS showed that changing the oxygen partial pressure did not change the stoichiometric formulation of the films, but it did change the number of W=O bonds at the grains boundary. We therefore suggest that the main effect of the oxygen, for the partial pressure range that we analyzed, is on the morphology of the films and not on their chemical composition.

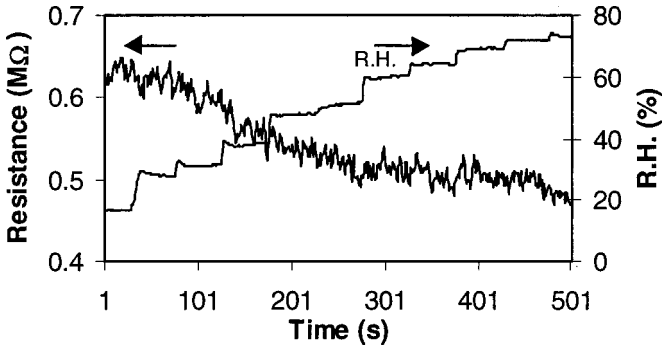

Figure 10. Typical response of gas (S4) sensor to humidity.

The annealing treatments induced a crystallization of the as-grown WO_3 amorphous layer. The Raman spectra recorded after annealing, compared with data reported in the literature,[18] suggested that the structure of the films was monoclinic. The ratio of integrated Raman scattering intensities (W=O/O-W-O) was used as a measure of the relative cluster size. The cluster size increased as annealing temperature increased. On the basis of the results found by XPS, AFM, SEM, and Raman spectroscopy the sensors were annealed at 350°C for 24 h. These devices were very sensitive and selective to NH_3 when operated at 250°C, slightly sensitive to ethanol and almost insensitive to other gases and vapors like benzene and methane. At this operating temperature, their water vapor cross sensitivity was moderate and typically lower than that of the commercially available gas sensors (*e.g.*, TGS-type). The sensor prepared with $Ar:O_2$ partial pressure equal to 1:1 showed the highest sensibility to NH_3. AFM and SEM revealed that it has the highest surface roughness and the smallest grains when annealed at 350°C compared with the other films. In principle, films with small grains should be more sensitive than films with bigger grains. This is because the surface area for interaction of the latter is lower.

Further work is needed to correlate the presence of the W=O bonds with the gas sensing properties of the material.

Acknowledgments

This work was partly funded by the Spanish Commission for Science and Technology (CICYT) under grant no. TIC-2000-1598-C02. The authors gratefully acknowledge Dr. L. A. O. Nunes and Dr. A. S. S. de Camargo for helpful discussions. C.B. is grateful to Fapesp for a fellowship

Universitat Rovira i Virgili assisted in meeting the publication costs of this article.

References

1. K. Cammann, *Sens. Actuators*, **6**, 19 (1992).
2. P. T. Moseley, *Sens. Actuators*, **6**, 149 (1992).
3. P. T. Moseley and B. C. Tofield, *Solid State Gas Sensors*, Adam Hilger, Bristol (1987).
4. J. W. Gardner and P. N. Bartlett, *Synth. Met.*, **57**, 3665 (1993).
5. W. Göpel, *Prog. Surf. Sci.*, **20**, 9 (1989).
6. P. T. Moseley, *Meas. Sci. Technol.*, **8**, 223 (1997).
7. M. Akiyama, J. Tamaki, N. Miura, and N. Yamazoe, *Chem. Lett.*, **1**, 1611 (1991).
8. J. Tamaki, Z. Zhang, K. Fujimori, M. Akiyama, T. Harada, N. Miura, and N. Yamazoe, *J. Electrochem. Soc.*, **141**, 2207 (1994).
9. E. Llobet, G. Molas, P. Molinas, J. Calderer, X. Vilanova, J. Brezmes, J. E. Sueiras, and X. Correig, *J. Electrochem. Soc.*, **147**, 776 (2000).
10. Y. Shigesato, Y. Hayashi, A. Masui, and T. Haranou, *Jpn. J. Appl. Phys., Part 1*, **30**, 814 (1991).
11. J. E. Germain, in *Adsorption and Catalysis on Oxide Surfaces*, M. Che and G. C. Bond, Editors, p. 335, Elsevier, Amsterdam, (1985).
12. S. Coluccia, A. Zecchina, G. Spoto, and E. Guglielminotti, *J. Chem. Soc., Faraday Trans. 2*, **79**, 607 (1983).
13. P. G. Harrison *et al.*, *J. Chem. Soc., Faraday Trans. 2*, **80**, 1341 (1984).
14. E. Llobet, X. Vilanova, J. Brezmes, J. E. Sueiras, R. Alcubilla, and X. Correig, *J. Electrochem. Soc.*, **145**, 1772 (1998).
15. C. Cantalini, H. T. Sun, M. Faccio, M. Pelino, S. Santucci, L. Lozzi, and M. Passacantando, *Sens. Actuators B*, **31**, 81 (1996).
16. J. C. Vickerman, Editor, *Surface Analysis—The Principal Techniques*, John Wiley & Sons, New York (1997).
17. M. F. Daniel, B. Desbat, J. C. Lassegues, B. Gerand, and M. Figlarz, *J. Solid State Chem.*, **67**, 235 (1987).
18. A. Rougier, F. Portemer, A. Quede, and M. E-Marssi, *Appl. Surf. Sci.*, **153**, 1 (1999).
19. T. Kubo and Y. Nishikitani, *J. Electrochem. Soc.*, **145**, 1729 (1998).
20. J. Gerblinger, U. Lampe, H. Meixner, I. V. Perczel, and J. Giber, *Sens. Actuators B*, **18-19**, 529 (1994).
21. J. Brockington and P. J. Stamper, *Inorganic Chemistry for Higher Education*, p. 214, Longman Group Ltd., London (1983).
22. G. Sberveglieri, S. Groppelli, P. Nelli, A. Tintinelli, and G. Giunta, *Sens. Actuators B*, **24-25**, 588 (1995).